LMSC
L-86-68-2
c-2-P

Lockheed

PALO ALTO RESEARCH LABORATORY

LOCKHEED MISSILES & SPACE COMPANY • A GROUP DIVISION OF LOCKHEED AIRCRAFT CORPORATION
PALO ALTO, CALIFORNIA

501-55810

ELECTROMAGNETIC SIMULATION OF MICROWAVE BACKSCATTER FROM THE OCEAN SURFACE: A FEASIBILITY STUDY

Robert B. Ward

L-86-68-2 June 1968

Prepared for
Astrionics Laboratory
George C. Marshall Space Flight Center
Huntsville, Alabama
Contract No. NAS 8-20395

Signal Processing Group
Electronic Sciences Laboratory
Lockheed Palo Alto Research Laboratory
LOCKHEED MISSILES & SPACE COMPANY
A Group Division of Lockheed Aircraft Corporation
Palo Alto, California

FOREWORD

This report was prepared for the Astrionics Laboratory of the George C. Marshall Space Flight Center, under Contract No. NAS 8-20395, by the Signal Processing Group of the Electronic Sciences Laboratory, Lockheed Palo Alto Research Laboratory.

CONTENTS

ILLUSTRATIONS

TABLES

Section 1
INTRODUCTION

Backscatter of microwave signals from extended random surfaces such as the ocean is a phenomenon of continuing interest. Radars contend with ground and sea clutter while radar altimeters and doppler navigators operate with uncertain ground and sea echo characteristics. Nevertheless, theoretical treatments (Refs. 1, 2, 3) of the scattering process still have a number of limitations. In addition to the deficiencies of knowledge with respect to existing equipment, recent interest has included the problem of conceiving and designing radar equipment with the objective of using the backscattered signals to measure some parameters of an ocean surface producing the backscatter (Refs. 4, 5, 6, 7).

The systems proposed for this use are concerned with near-vertical incidence whereas earlier interest was mainly in angles near grazing. Finally, the new systems propose to use depolarized backscattering, multifrequency, and other approaches which should be examined experimentally before equipment development is begun.

Experimental approaches to the problem have heretofore mainly consisted of measurements of microwave backscatter made in the field on actual or representative surfaces (Ref. 8). Some of these measurements have been made from aircraft, some from bridges, hilltops, etc., but common drawbacks have been:

- Quantitative measurements of the parameters of the scattering surface often have not been made. Even when surface conditions were measured, the measurements were generally not sufficiently detailed. That is, the entire spectrum of the surface from very long to very short wavelengths was not measured. Finally, at times the surface measurements taken were not from the same portion of the surface where the scattering was measured or were not made at the same time the scattering was measured.

- The scattering measurements were made of those surfaces nature served up to the experimenters.
- Field tests limit the ability of the experimenters to vary the parameters of the experiment at will in order to study the effect of parameter changes.
- Field tests are notoriously expensive, complicated, and time consuming for the amount of real information obtained.

These factors have limited the extension and completion of analytic treatments of the problem.

Attempts at simulation of microwave scattering from rough surfaces have been rather limited. One technique has used ultrasonic acoustic waves in water (Ref. 9). Another recent attempt was the use of microwave acoustics in crystalline media (Ref. 10). Both of these suffer from the fact that acoustic wave propagation is not governed by the same equations as electromagnetic wave propagation, and in particular the polarization property is missing.

Another deficiency of available data is due to the fact that radars are now beginning to operate from satellites, rather than only from the surface and from aircraft. This factor changes the surface area covered by a beam of fixed angle by orders of magnitude.

Based on these considerations, it is desirable to attempt a simulation in which electromagnetic radiation is used and the dimensions of the problem are scaled down to laboratory or test-range size. In such a case, electromagnetic radiation at some shorter wavelength will be used and the dimensions of the surface as well as the radar-surface separation will all be decreased by the ratio of the microwave wavelength being simulated to the wavelength used in the simulation. An illustrative operational case is shown in Fig. 1, along with a conceptual sketch of the simulation approach. In this figure, a low-orbit satellite transmits microwave energy earthward and receives backscattered return from portions of the surface out to perhaps 45 deg from the nadir. By the use of a narrow beam or by range-doppler processing, the satellite isolates the

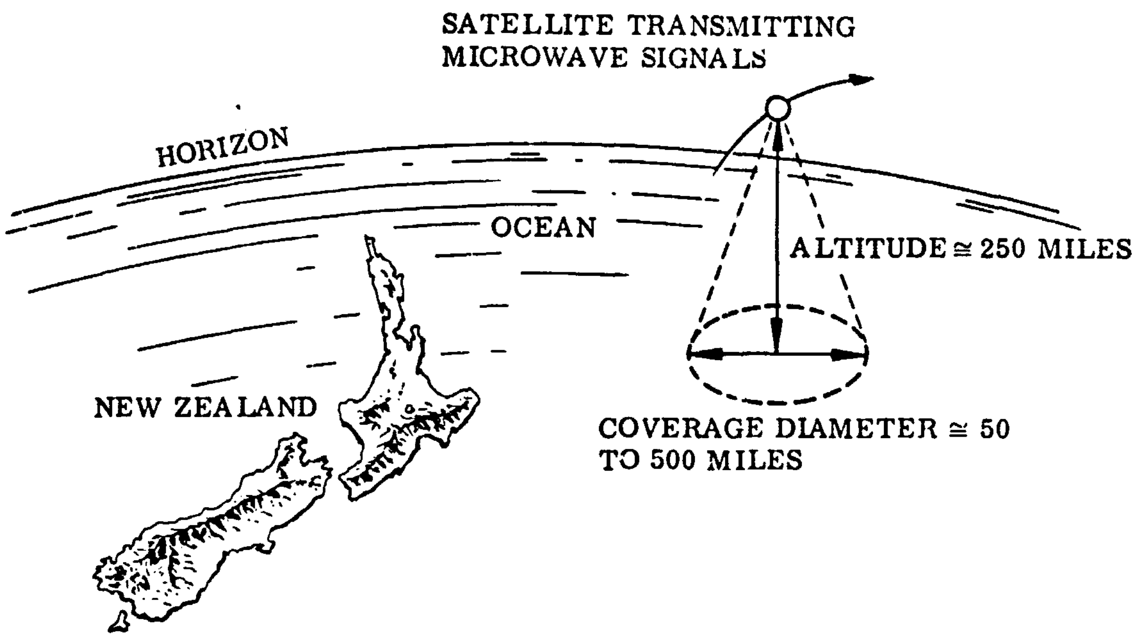

a. Approximate Radar Situation To Be Simulated

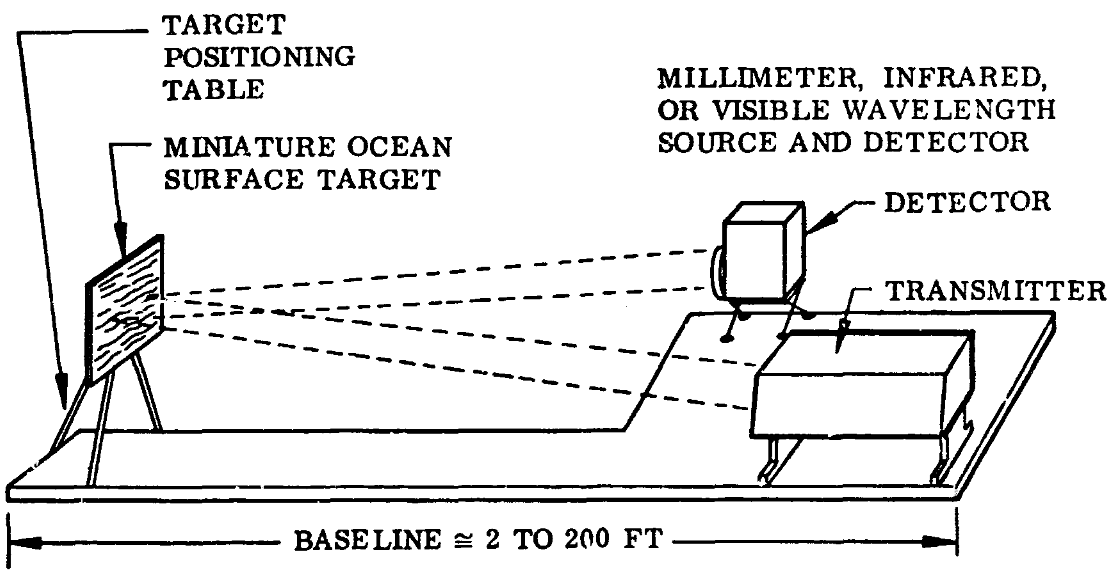

b. Basic Laboratory Simulation Concept

Fig. 1 Simulation of Microwave Scattering From the Ocean signal associated with a particular resolution cell on the surface. The dimensions of such a cell are usually not small; perhaps on the order of 200 to 20, 000 ft. Therefore, a simulation must account for backscatter from a moderately large element of surface having a range of incidence angles of about ± 45 deg. How this is simulated is shown simply in Fig. 1b where the target size corresponds at least to the 200- to 20, 000-ft radar resolution cell, the baseline corresponds to the altitude, and the various incidence angles are obtained by tilting the target.

This report presents the details of a study into the feasibility of such a simulation. The primary questions to consider are, "What wavelength should be chosen for the simulation source?," and "What is a suitable technology for fabricating the scattering surfaces so as to represent a desired ocean surface?" After sufficient justification, it is shown that the best present course is to choose 10.6 μ for the simulating wavelength and to fabricate the scattering surface by a light-activated chemical engraving process. Based on both analysis and limited experiments performed during the feasibility study, it appears that it should be feasible to simulate the operation of a 500-MHz scatterometer operating at 200- to 400-km altitude and scattering signals off nearly a square mile of ocean surface.

Some results are presented on methods of measuring the parameters of miniature target surfaces, however fabricated. Finally, a scattering simulation facility using a 10.6-μ CO_2 laser set up in the Lockheed Palo Alto Research Laboratory is described and some initial results from it are given.

Section 2
CONSIDERATIONS IN CHOICE OF SIMULATING WAVELENGTH

2.1 MICROWAVE FREQUENCIES OF INTEREST

The problem of immediate interest is that of a satellite-borne radar altimeter, scatterometer, or sea-surface-sensing device. Therefore, microwave frequencies of interest could possibly extend from the ionospheric critical frequency (8 to 20 MHz) up beyond K-band and even include the windows at 35 GHz and 95 GHz. However, realistically, the lower frequency limit is probably set by excessive ionospherically caused effects at somewhere in the neighborhood of 300 to 400 MHz. The upper frequency of interest is probably set by excessive weather attenuation at about 15 GHz.

2.2 DIMENSIONS OF THE SURFACE TO BE SIMULATED

Another consideration in the choice of microwave frequencies of interest is the purpose of the radar. When used for sea-surface-sensing, the frequency ideally should be associated with the dimensions of the surface of interest. Since the ocean surface consists of dimensions from small ripples with centimeter wavelength all the way to long gravity waves with wavelengths of 500 to 1000 ft, ideally all radar frequencies from 300 MHz to 15 GHz are candidates for consideration. At present, NASA has two experimental aircraft-borne scatterometers in operation, one at 13.3 GHz (Ref. 11) and one at 400 MHz.

The dimensions of the sea surface we wish to simulate also bear most strongly on the requirements for making the target surface. It would be desirable to reconstruct a miniature ocean surface in exact detail. However, when the problems of constructing a surface are examined closely, it soon becomes apparent that unless the amount of surface detail is restricted, the problems of target construction become insurmountable.

The choice of simulating wavelength, the choice of target construction method, and the choice of target dimensions to include in the simulation become strongly interrelated on this point.

In fact, the target problems are so difficult that the microwave frequencies for initial consideration are restricted to the low frequency end of the band. Therefore, it was decided for this program to emphasize a radar frequency of 500 MHz. This is near the 400-MHz frequency now in use by a NASA scatterometer so a simulation at this frequency would be significant. At the end of this program it should be possible to be more specific as to the high frequency limit of a simulation of this type.

The emphasis so far has been on the fine detail of the surface. The extent of the surface also enters the picture. The longest wavelength ocean waves are 500 to 1000 ft. If we wish to produce surfaces which average a number of these long waves, the horizontal extent of the surface to be simulated is thousands of feet. If this is to be reproduced as a target with convenient dimensions for an experiment, a scaling factor somewhere between 10^2 and 10^5 will have to be applied. When 500 MHz (60 cm) is scaled by these factors, the simulating wavelengths of interest lie in the range from 6 μ to 0.6 cm.

2.3 AVAILABILITY OF SOURCES AND DETECTORS

Unfortunately, at this time the range of 6 μ to 0.6 cm, is largely a no-man's land as far as coherent sources are concerned. It extends from millimeter waves through a large portion of the infrared. Only at the ends are coherent sources available. Millimeter wave sources exist up to about 500 MHz (0.6 mm). The infrared CO_2 laser is the only coherent source commercially available at present at the other end of the range (10.6 μ). However, there is a good possibility that within the next year or two, water vapor lasers operating at 30 μ or 100 μ will be available. Thus, the techniques under investigation may be applied to other radar frequencies at that time.

(At this point, the possibility using the near infrared or visible lasers might be raised. As will be demonstrated later, the target fabrication problems become impossible in that range.)

Detectors are available for both the millimeter and infrared regions of interest although sensitivities are not the best. The infrared detectors are generally photoconductive detectors using cryogenically cooled semiconductors. They are all incoherent detectors, although perhaps coherent detection might be possible by using as a reference a portion of the transmitted 10.6-μ signal. The millimeter wave detectors may be either mixers or power detectors so that coherent operation in this wavelength region is possible. This could be a real advantage if such measurements are found to be desirable and the IR detectors cannot be operated coherently.

2.4 QUANTUM CONSIDERATIONS

The simulating wavelength must be chosen so that the electromagnetic wave reflections at the air-target boundary occur in the same way that the microwave-ocean surface reflections occur. That is, the reflection must be governed by the conductivity and dielectric constant of the target rather than being subject to any quantum interactions. The latter might occur if visible light were used with certain target materials. The longer the wavelength, the less problem this factor poses. At 10.6 μ all but the most special materials will result in reflections directly analogous to microwave reflections.

2.5 FUNDAMENTAL PROBLEMS IN TARGET CONSTRUCTION

2.5.1 Basic Approach: Deterministic or Random

The first question to face in examining the problems of target construction is general: "Should the target be made by some random process (for example, sandblasting), or should it be made point by point to some specification or description?" While the first case has the advantage of simplicity, it would be necessary to find some process which would approximate the sea surface. This is not easy. The sea surface is not simply random piles of water, but results from the summation and interaction of waves traveling in various directions and having a number (or more nearly a continuum) of wavelengths and amplitudes. The spectrum (Fig. 2) consists of a concentration of

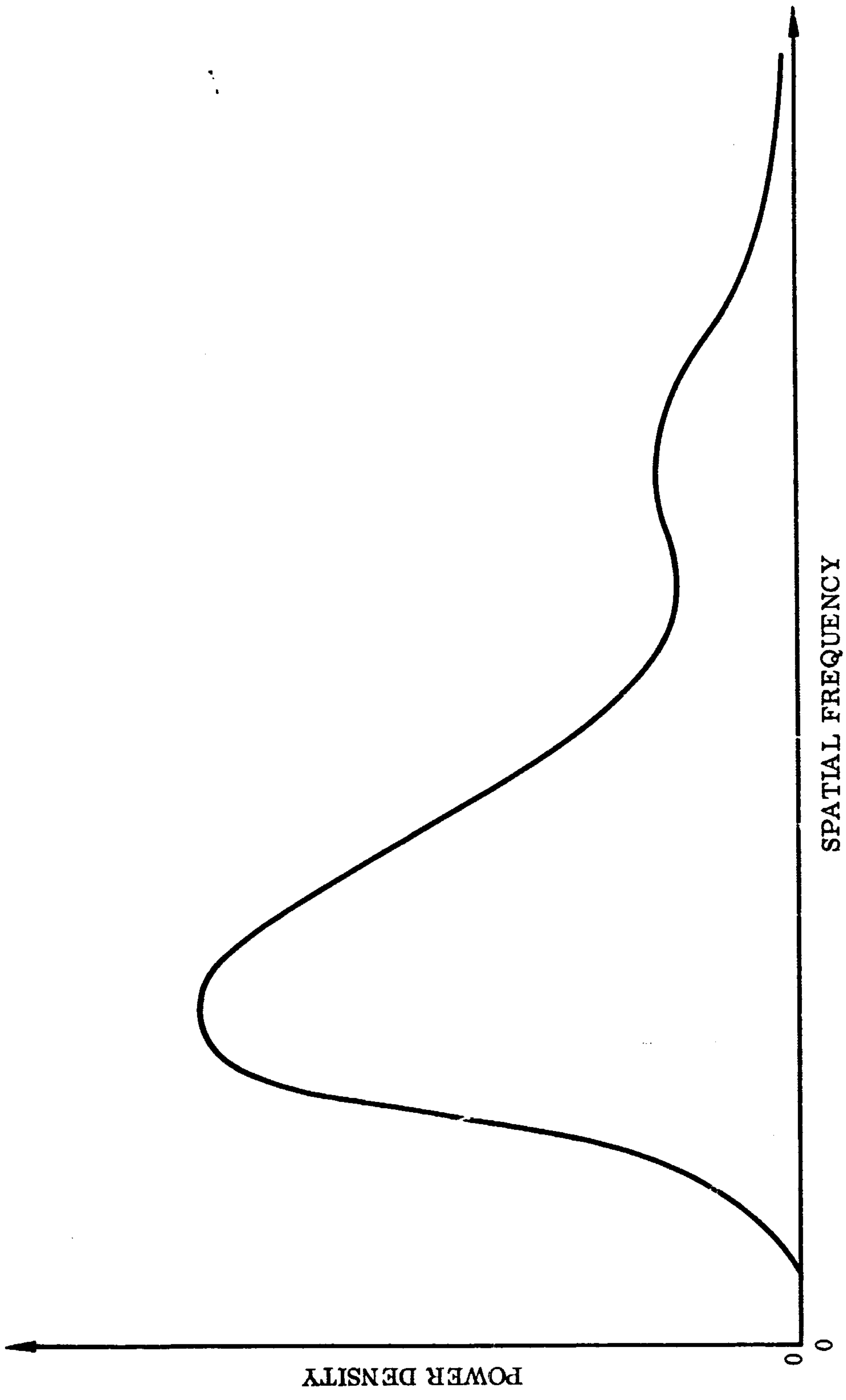

Fig. 2 Typical Ocean Surface Spectrum

energy at a medium wavelength with diminishing amounts of energy toward the shorter and longer waves. Secondary maxima are often observed at higher frequencies. The spectrum changes under the influence of winds, both local and remote.

If the deterministic approach is followed, the surface height is specified point by point in accordance with a desired sea condition and means found to make the replica have that same height function in miniature. This is a very powerful approach since it enables nearly exact control over the experimental situation. Surfaces could be realized having just the character desired (amplitude, spectrum, isotropic or not, etc.). Of course, this approach requires an extremely delicate and ingenious approach to target manufacture.

The choice of basic approach must be considered carefully. Some estimates have to be made of the best that can be done in target fabrication, for example. The course that was adopted early in the feasibility study was to press for the deterministic approach and it now appears that this will be successful. Because considerable time is required for the target fabrication techniques to be fully worked out, random targets were planned for initial test of the scattering simulation experiment.

2.5.2 Target Construction Time

When considering ways to prepare a target surface, possibly the first approach that comes to mind is some form of precision machining. Suppose the desired surface height, Z, has been specified as a function of horizontal position

$$Z_{ij} = f(x_i, y_j) \tag{1}$$

for $i, j = 1, 2 \ldots M$. We might think of sculpturing the surface out of a blank piece of material by milling a square hole of width $x_k - x_{k-1} = y_k - y_{k-1}$ down to the height Z_{ij} and sequentially doing this for each point (i, j) in the matrix. How long might this take?

The number of points in the matrix depends on the horizontal extent of the surface to be simulated and the amount of detail we include. Because the longest ocean waves are 500 to 1000 ft, to include a number of these waves the horizontal extent must be at least several thousand feet and 5000 feet seems to be adequate. If the radar wavelength being used is 60 cm (500 MHz), then a height resolution of about $\lambda/10 = 6$ cm is needed. Since the slope of the sea surface rarely exceeds 20%, a horizontal resolution of 30 cm or about 1 ft should be adequate.

Therefore, sufficient horizontal extent and detail for 500 MHz can be obtained by a matrix of 5000 × 5000 points. Considerably less inclusive but still useful might be a horizontal extent of 500 ft with the same detail, thus requiring a matrix of 500 × 500 points. Table 1 lists the total target fabrication times for both 500- and 5000-ft horizontal extent when the matrix elements are sequentially made.

Table 1

TARGET FABRICATION TIME FOR 500-MHz SIMULATION

	Total Time	
Time per Element	500-ft Target	5000-ft Target
10 sec	33 days	9 yr
1 sec	78 hr	330 days
0.1 sec	7.8 hr	33 days
10 msec	47 min	78 hr
1 msec	4.7 min	7.8 hr
100 μsec	25 sec	47 min
10 μsec	2.5 sec	4.7 min

It is apparent that if any sequential operations are to be used, the time per operation must be quite small, probably 10 msec at a maximum and preferably much less. If the same analysis is applied to an X-band simulation, which would require 400 times the surface detail, results are even more striking. They are shown in Table 2.

Table 2

TARGET FABRICATION TIME FOR 10-GHz SIMULATION

Time per Element	Total Time 500-ft Target	5000-ft Target
1 sec	3.6 yr	360 yr
0.1 sec	132 days	36 yr
10 msec	13 days	3.6 yr
1 msec	1.3 days	130 days
100 μsec	3.1 hr	13 days
10 μsec	19 min	1.3 days
1 μsec	1.9 min	3.1 hr

The time consideration leads to the following conclusions:

- Mechanical methods of fabrication are completely out of the question for a 10-GHz simulation and are only remotely possible for a 500-MHz simulation.
- Fabrication methods which operate on all matrix points simultaneously are desirable. This suggests the use of an optical approach.

2.5.3 Optical System Limitations on Detail

The fundamental limitation on resolution in an optical system was shown in 1834 by Sir George Airy to be:

$$d = 2.44\lambda \text{ (F number)} \qquad (2)$$

where d is the diameter of a focused spot to the first dark ring, λ is the wavelength of light being used, and (F number) is the ratio of lens focal length to aperture. If $\lambda = 0.5\mu$ (visible) and a good lens of f2 is being used, the spot diameter $= 2.44\mu$. While a slightly better lens might be possible and ultraviolet light might be used, an often used rule of thumb with photographers is that the best resolution is obtained when a lens is stopped down one or two stops. This would tend to offset any gains made. The conclusion still remains that a practical resolution limit for optical processes lies somewhere in the range 1 to 3 μ.

2.5.4 Materials and Process Limitation on Resolution

If a piece of material is to be contoured to form a surface, it should first be very flat. In optical work it is common to prepare a surface flat to 1/10 the wavelength of optical light or about 0.06 μ.

Imperfections in the material will tend to form a fine-textured surface as the surface is contoured. These can be the results of dislocations in crystals, impurity centers, etc. It is estimated that such texture can be held to near 1 μ.

2.6 TARGET DIMENSIONS AS A FUNCTION OF SIMULATING WAVELENGTH

Tables 3 and 4 present the important dimensions of the target when various wavelengths are used for the simulating signal. The surface extent considered is again either 500 or 5000 ft. The largest height variation is 50 ft corresponding to very high sea.

Table 3

TARGET DIMENSIONS FOR 500-MHz SIMULATION

Simulating Wavelength	Target Dimensions							
	Horizontal Size Simulating		Vertical Displacement Simulating		Horizontal Resolution Simulating	Source-Target Spacing to Simulate Altitude		
	500 ft	5000 ft	6 cm	50 ft	30 cm	200 km	400 km	10 km
0.63 μ	0.16 mm	1.6 mm	0.06 μ	16 μ	0.3 μ	21 cm	42 cm	1.06 cm
3.39 μ	0.86 mm	8.6 mm	0.34 μ	86 μ	1.7 μ	1.1m	2.3 m	5.7cm
10.6 μ	2.69 mm	2.69 cm	1.06 μ	269 μ	5.3 μ	3.5 m	7.1 m	18 cm
0.6 mm (500 GHz)	15.2 cm	1.52 m	60 μ	1.52 cm	300 μ	200 m	400 m	10 m
3 mm (100 GHz)	76.3 cm	7.63 m	300 μ	7.62 cm	1.5 mm	1000 m	2000 m	50 m
8 mm (35 GHz)	2.04 m	20.4 m	0.8 mm	20.3 cm	4 mm	2.7 km	5.3 km	130 m

LOCKHEED PALO ALTO RESEARCH LABORATORY
LOCKHEED MISSILES & SPACE COMPANY
A GROUP DIVISION OF LOCKHEED AIRCRAFT CORPORATION

Table 4

TARGET DIMENSIONS FOR 10-GHz SIMULATION

Simulating Wavelength	Target Dimensions							
	Horizontal Size Simulating		Vertical Displacement Simulating		Horizontal Resolution Simulating	Source-Target Spacing to Simulate Altitude		
	500 ft	5000 ft	0.3 cm	50 ft	1.5 cm	200 km	400 km	10 km
0.63 μ	3.22 mm	3.22 cm	0.06 μ	320 μ	0.3 μ	4.2 m	8.4 m	21 cm
3.39 μ	1.72 cm	17.2 cm	0.34 μ	0.17 μ	1.7 μ	23 m	46 m	1.1 m
10.6 μ	5.4 cm	54 cm	1.06 μ	0.54 cm	5.3 μ	71 m	142 m	3.5 m
0.6 mm (500 GHz)	3.05 m	30.5 m	60 μ	30.5 cm	300 μ	4 km	8 km	200 m
3 mm (100 GHz)	15.2 m	152 m	0.3 mm	1.52 m	1.5 mm	20 km	40 km	1 km
8 mm (35 GHz)	39.7 m	397 m	0.8 mm	3.97 m	4 mm	54 km	108 km	2.7 km

The simulating wavelengths in these tables correspond to various possible sources. Visible and infrared lasers are available at 0.63, 3.39, and 10.6 μ. After 10.6 μ there is a gap until the highest frequency millimeter wave sources are reached.

These dimensions allow us to begin narrowing down the possible simulating wavelengths. Primary consideration is given to the 500-MHz simulation since it is the first to be attempted. The visible wavelength (0.63 μ) is out of the question because the target size is too small and the resolutions are not achievable. The 3.39-μ infrared wavelength is probably just beyond the resolution achievable and the size is a little too small for convenience.

At the other end of the scale, the size of the target (67 ft) is so large at 8-mm wavelength that building the support towers to hold and rotate it would be excessively expensive. Even at 3 mm the target size is 25 ft to represent a 5000-ft surface. Source-target spacing to simulate satellite altitude is also so large that an outdoor range would have to be set up. The spacing factor is probably not very significant in the simulation so that by the time 0.6 mm is reached, the separation could be ignored and the target size is small enough to allow an indoor facility (although it would require at least partly anechoic quarters).

With this background, the final choice appears to lie between the 10.6-μ laser and the 500-GHz millimeter wave source. The 10.6-μ laser was selected for the following reasons:

- 500 GHz is presently an experimental outpost of the millimeter region whereas a number of CO_2 lasers are available with plenty of power at 10.6 μ.
- It appears likely that water vapor lasers will be available in the next year or two. These will operate at 30- to 100-μ wavelength and would provide a satisfactory simulation at higher microwave frequencies with the same target resolutions presently estimated for the 500-MHz simulation.
- Target fabrication using optical techniques can be done for the 2.7-cm target size corresponding to a 10.6-μ simulation wavelength so that the target fabrication time problem can be overcome. Optical problems in trying to make the 5-ft target associated with a 0.6-mm simulation wavelength would be severe.

Section 3
A SURVEY OF MICROSURFACE FORMING TECHNIQUES

3.1 THE OVERALL DETERMINISTIC APPROACH

In the deterministic approach to target fabrication, we start with the assumption that there exists, stored in some recorded form, information which describes the desired height of a surface Z_{ij} at each of a large number of points X_i, Y_j. We also assume that this information can be read out quite rapidly, at say 10^4 to 10^6 points per second.

There are three general deterministic approaches to target fabrication:

(1) Sequential. Here the desired height for point 1 is read from the memory and the height of the first point of the target surface is set. The next point is then read from memory and the second point of the target surface is set, and so on, until the surface is complete. Examples of sequential approaches studied are:

Mechanical machining
Laser machining
Electron beam machining

Such approaches are generally slow.

(2) Parallel. Here the height function is read rapidly from memory and stored in a form such that it can, in a later step, construct all points of the surface simultaneously. Typically, the intermediate storage is in the form of a photographic negative where the transmissivity of light at each point X_i, Y_j of the film represents the corresponding desired surface height. When such a negative is imaged on a surface, the desired height is a function of light intensity. Choice of a surface-forming method sensitive to light intensity would then complete the process. Examples of parallel approaches studied are:

Thermoplastic recording
Photochemical etching

Photo sublimation
Photo epitaxial growth
Other photo chemical

(3) Combined Sequential-Parallel. In this case the height function is read out rapidly into a series of intermediate storages each suitable for parallel formation of a part of the surface. For example, suppose a high contrast photonegative is made where only two levels, black and clear, are used. If black represents all surface points whose height is greater than Z_o, the minimum point of the surface, this first negative is all black. The next negative is made where black represents all surface points whose height is greater than $Z_o + 1\ \mu$. In the following negative, black corresponds to $Z > Z_o + 2\ \mu$, and so on, until a totally clear negative is obtained. If each of these negatives can now be used to result in parallel growth (or reduction) of those surface points which are clear (or black), then the total number of steps of surface fabrication is intermediate between the M^2 steps of the sequential approach and the single step of the parallel approach. Examples of combined approaches are:

Multilayer deposition
Multilayer etching

3.2 MECHANICAL MACHINING

In this method, a fine point would cut a surface in a manner similar to the cutting of a phonograph record. Methods other than rotating would be necessary for transporting the work under the cutting head. The finest diamond stylus used in profile measuring instruments (Refs. 13, 14) has a tip radius of 2.5 μ. Positioning of the work under the cutting tip could conceivably be done to a tolerance of $\pm$ 0.0001 in. = $\pm$ 2.5 μ.

Ruling machines for optical diffraction gratings produce 15,000 lines per inch or so, which is about three times our requirement. However, the development of a machine capable of doing such a job would no doubt be a major undertaking. Finally, this would be a relatively slow sequential process, probably not capable of more than 100 to 1000 matrix points per second.

3.3 LASER MACHINING

A number of companies are now producing laser machining equipment (Refs. 15, 16, 17). This technique is mainly used for drilling holes and cutting patterns, fine trimming, etc. Very little if any use has been made of such instruments for surface contouring as yet.

Laser light focusing has the same limitation due to the wavelength and the lens f-number as does microphotography. This limit is the range 1 to 3 μ for visible lasers. However, present equipment appears to be limited to around 10 μ. Control of depth of cut to the 1 μ desired is not presently possible nor is any good estimate of depth accuracy available. A final drawback is that even the so-called high-pulse-rate lasers operate at 60 pulses per second and, even if each pulse could be set to drill one matrix point, the operation would be sequential at 60 matrix points per second.

It is conceivable that cw lasers could be used for such machining and the speed of the work under the laser spot be varied to adjust the depth of cut. However, this would involve major development.

Two organizations specializing in laser machining systems (Lear Siegler Laser Systems Center, Ann Arbor, Michigan, and American Optical, Pittsburgh) were contacted and asked to comment on the possibility of laser machining a surface to the following specifications:

Area:	1/2 by 1/2 in.
Horizontal Resolution:	3 μ
Vertical Resolution:	1 μ
Maximum Depth:	250 μ
Maximum Surface Slope:	33%

Both groups replied that it was not presently feasible, especially because of the 1-μ depth requirement.

3.4 ELECTRON BEAM MACHINING

Electron beams are used for welding and cutting (Refs. 14, 18) in much the same way as lasers. Except that the work must be in a vacuum, the capabilities are similar. The Hamilton-Zeiss Model CW-1 provides a focused spot of 12- to 25-μ diameter. This machine is quite complete and by addition of automatic programming could probably be made suitable for contouring a surface. It would still be sequential operation and would only give 12.5-μ horizontal resolution and unknown depth resolution.

3.5 THERMOPLASTIC RECORDING

This is a technique (Ref. 19) developed for recording in which electrons are deposited on the surface of a flat plastic sheet in accordance with a desired surface height. Because the plastic is nonconductive, the electrons stay where they have been deposited while the plastic is heated. The soft plastic is then placed in an electrostatic field where the surface electrons are subjected to electrostatic forces. The surface of the soft plastic is thereby deformed more where the electron density is large and less where it is small.

The General Electric Laboratories at Syracuse, where this research has been conducted, were contacted for their appraisal of the applicability to surface contouring. Present work uses only 10-μ thick plastic and produces 1-μ deformation. Since the effects are inverse squared, the liklihood of obtaining anything like the 250-μ peak-to-trough separation desired is extremely remote.

3.6 PHOTOCHEMICAL ETCHING

In this method, a negative is first made in which the transmissivity represents the desired height function. When the image is focused on a semiconductor in an etching solution, electron-hole pairs are created in the semiconductor. They may react with the etchant to remove an atom of the semiconductor. The intensity of the light determines the density of electron-hole pairs and consequently the amount of material etched away from the surface.

The limitations of this method with respect to resolution are determined by:

- Optical resolution limits
- Mechanical vibration limits of the optical system
- Turbulence in the etchant since the image passes through it
- Properties of the semiconductor material such as diffusion constant, lifetime, impurity density, fault density, etc.

This is the most successful of several methods chosen for feasibility experiments, the results of which are detailed in a later section of this report. Briefly, a horizontal resolution of about 10 μ was demonstrated with equipment which leaves much room for improvement. Capability to etch to a depth of 250 μ in a reasonable time was also demonstrated.

3.7 PHOTO SUBLIMATION

This approach also begins with the imaging of a light intensity pattern representing surface height onto an initially smooth surface. However, in this case, the material is chosen to be one which sublimes at near room temperature and is in a vacuum. The light which enters the surface is absorbed in a very short distance in the material resulting in a temperature pattern of the surface atoms similar to the light intensity pattern. More sublimation takes place from high temperature than low temperature areas, thus contouring the surface.

This method was also selected for feasibility experiments but was not as successful as photo etching. The experiments will be described fully in a later section.

3.8 PHOTO EPITAXIAL GROWTH

In this proposed method (Fig. 3), silane gas at very low pressure was drawn into a cell past ionizing electrodes. The hope was that the silicon ions would be deposited on the surface of the silicon substrate most heavily where the light produced low conductivity paths through the substrate and thus build up the desired contour. In a very limited number of experiments, no measurable success was obtained in contouring the surface dependent on light intensity. Further experiments were not performed since photochemical etch methods were proving successful.

3.9 OTHER PHOTOCHEMICAL METHODS

The Special Applications Division of Eastman Kodak Company was contacted to see if any of their developments would be applicable to the surface-forming problem. No technique they were aware of could meet both the required resolution and range of surface height.

Kodak has available a glass called Fotoform which is made sensitive to etching by exposure to light. However, the process is a go-no-go proposition suitable for making holes rather than contouring.

Another method Kodak has described (Ref. 20) is one in which suitable chemical treatment of the emulsion during development of an exposed film plate produces a surface contoured in accordance with the exposure. However, the maximum height variation which could be obtained by this method is only about 5 μ.

3.10 MULTILAYER ETCHING

In this suggested technique (Fig. 4), a number of masks are first made, each of which is opaque in areas where the surface is to be higher than some fixed value. The fixed value is different by a small amount, say 1 μ, for successive masks. A

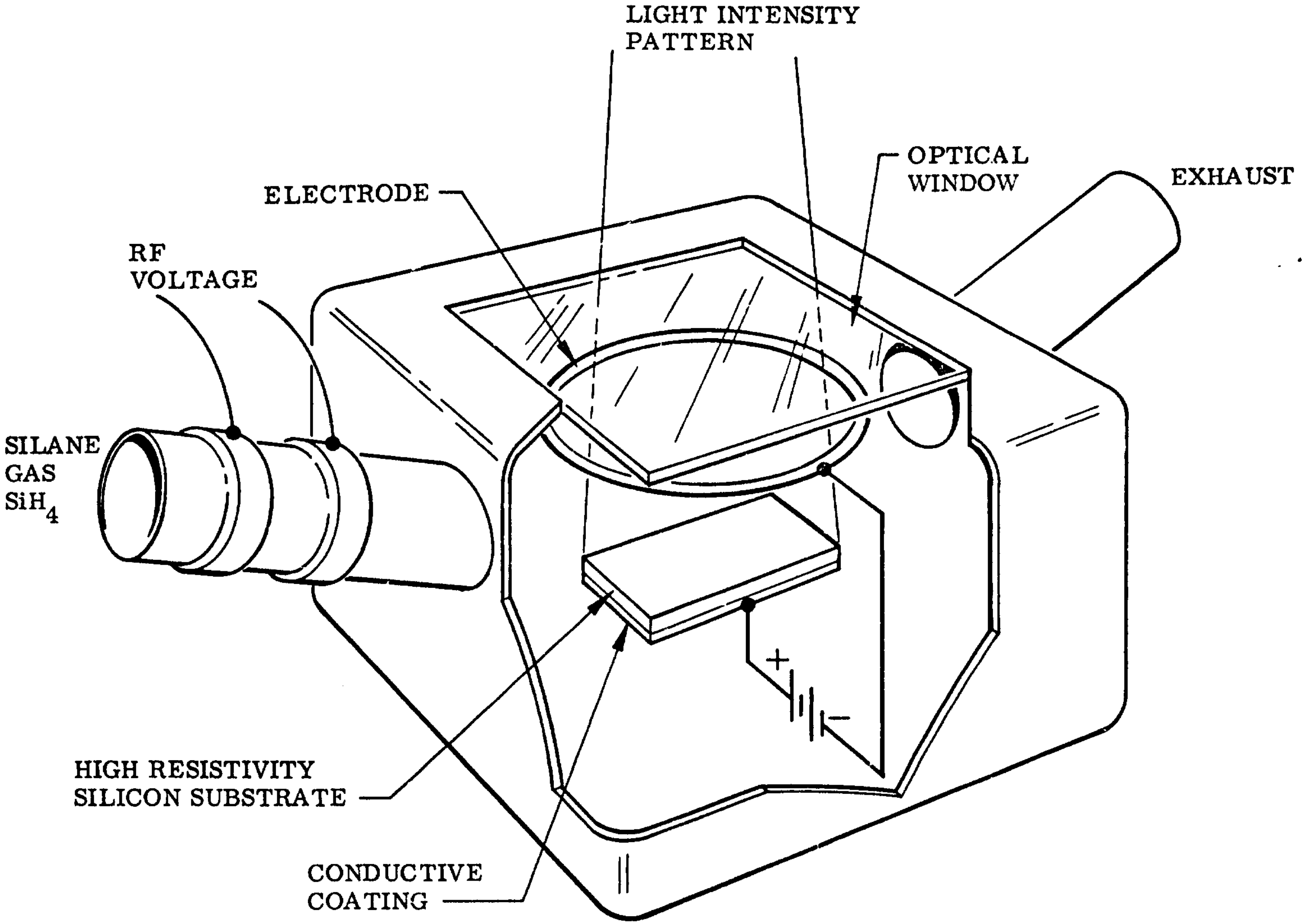

Fig. 3 Cell for Experiments in Photo Epitaxial Growth

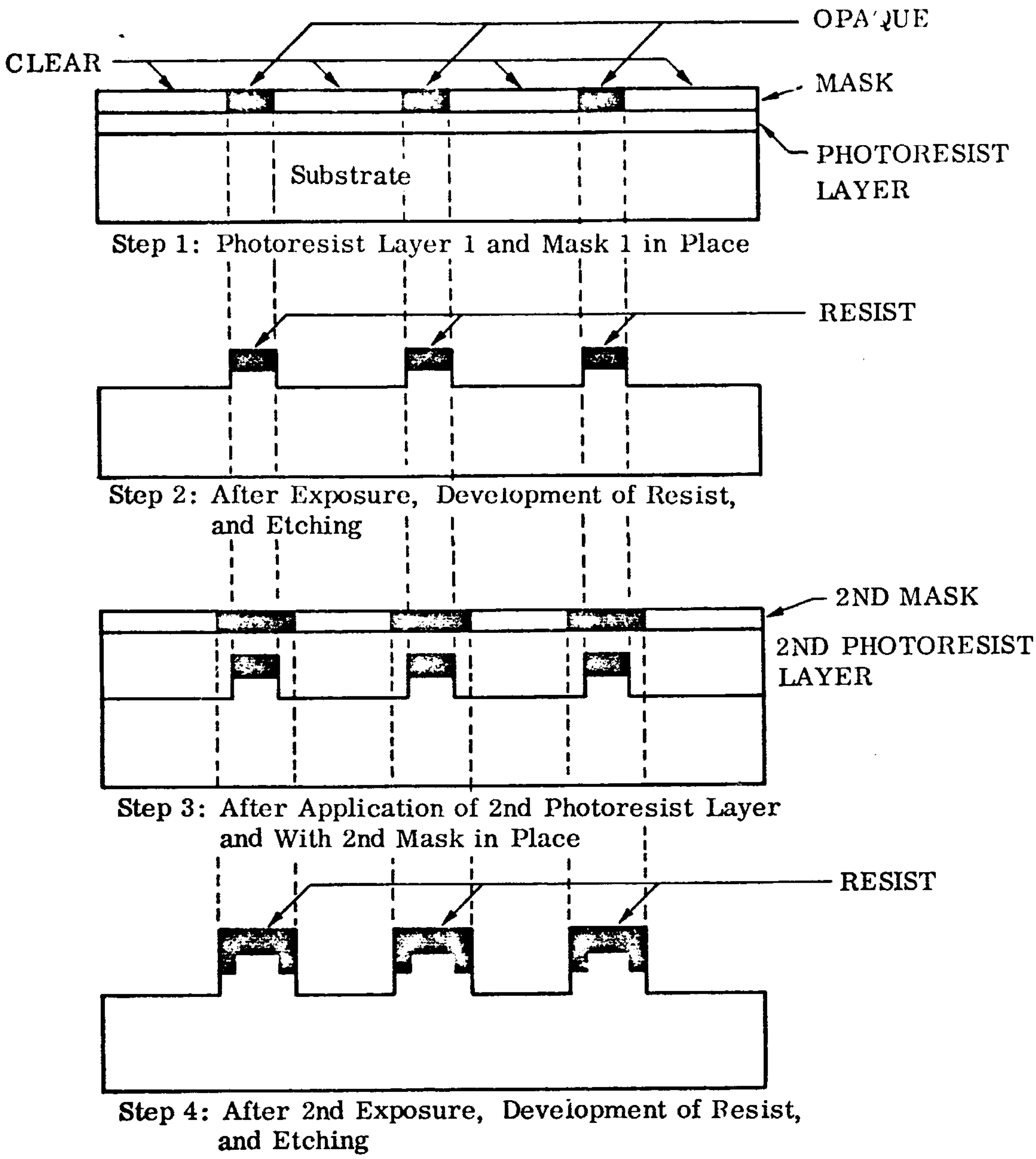

Fig. 4 Multilayer Etching Technique

photoresist layer is applied to the flat surface of the substrate and exposed through the first contact mask. After the photoresist layer is developed and the exposed portions washed off, etching away of 1 μ leaves small islands corresponding to the desired highest points of the surface.

A second photoresist layer is applied, masked with the second mask, and after the exposed resist is removed, a second 1-μ etching leaves two-stepped islands. This procedure is continued until the 250th layer is etched.

This technique is not the common photoresist technique used in the semiconductor industry where only a single resist layer is used. An LMSC group is producing single layer work having 1-μ resolution. No experiments were tried to determine the practical limitations of this method but presumably the problem of correctly registering each successive mask would be one of the most difficult limitations. Another drawback to such a method is that each step is rather long since the resist must be baked dry after each development so that to go through 250 steps would take several months.

3.11 MULTILAYER DEPOSITION

This method is essentially the reverse of the multilayer etching approach. Successive layers of photoresist are added to reduce the open plating area. The problems are the same as the multilayer etching approach and no experiments were made on this technique.

Section 4
RESULTS OF SOME EXPERIMENTS IN MICROSURFACE FORMING

By Robert D. Wales

4.1 PHOTOCHEMICAL ENGRAVING

4.1.1 Summary

An empirical relationship between light intensity, I, engraving time, t, and engraving depth x has been determined to be $x = 0.0625\ t^{1.18} \ln I/1.6$ for 0.5 to 1.5 Ω-cm n-type silicon oriented in the 1-1-1 plane and $x = 4.91 \times 10^{-4}\ t^{2.53} \ln I/54.5$ for 190 to 225 Ω-cm n-type silicon oriented in the 1-0-0 plane. The 1-1-1 silicon gave a surface having relatively large terraces which are probably due to the effect of orientation. The 1-0-0 silicon gave relatively small pits which are characteristic (initially) of dislocation pits. The resolution on the 1-0-0 silicon was better than 12 μ with the lens system used.

4.1.2 Introduction

It had been proposed that a sea surface replica be formed on a material which would allow the reproduction of a 1-square-mile surface on a 1-square-inch surface. Of the several techniques possible, the most feasible technique appears to be a light-activated deposition or removal of material on or from the replica surface. Since several materials exhibit a light-sensitive solution or etching effect, particularly n-type semiconductor materials, it appears that such materials can be utilized in the proposed application.

The effect of light upon semiconductor materials has been observed and examined to some extent (Refs. 21–29). Photoelectrolysis has been described by Uhlir (Refs. 22, 23, 29) and applied to device manufacture (Refs. 25, 28). The use of strong illumination is necessary, or aids, in the etching or polishing of many semiconductor materials, particularly n-type silicon (Ref. 24). Light-induced current multiplication has been studied and theory developed for instantaneous effects (Refs. 21, 23). Muller (Ref. 26) has determined the photovoltage of 0.5 to 60 Ω-cm n- and p-type silicon versus light intensity, while Braun (Ref. 27) utilized light to etch patterns in 0.1 to 100 Ω-cm n- and p-type silicon. However, the effects of light intensity and exposure time have not been studied.

The purpose of this study was to determine the feasibility of forming a complex replica by photochemical engraving, and to indicate the effects of the various parameters.

4.1.3 Experimental Procedure

The tests were performed on n-type silicon of 190 to 225 Ω-cm resistivity from Knapic Electro-Physics, Palo Alto, California, and 0.5 to 1.5 Ω-cm resistivity from Elmat, Mountain View, California, cut on the 1-0-0 and the 1-1-1 planes, respectively.

Before use, the silicon was immersed in White etch (Ref. 24) (1 HF/3 HNO_3) for about 2 min to obtain a polished surface. The photoengraving was performed in Dash etch (Ref. 30) (1 HF/3 HNO_3/10 HA_c).

The source of illumination was a General Electric 1000-W theatrical spotlight, and the patterns used were a solar critical focusing chart (Burke and James, Inc., Chicago, Illinois), a normal photographic step gauge, and a mask with a 21-mm-square opening.

The lens system consisted of an 8-in.-diameter glass plano-convex lens with a focal length of 14 in. placed about 1/2 in. after the pattern and about 28 in. from the light source. Further reduction was obtained with either a Wollensak f4.5 Enlarging Velostigmat 3-1/2 in. focus or a Wollensak-Dumont CRO 75 mm f1.9 Oscillo-Anastigmat No. C15413 lens.

The light intensity through the lens system to the silicon substrate was measured with a Spectra-Physics 4018 Power Meter 6328 Å. The photographs of the engraved patterns were taken under extremely oblique illumination to enhance the pattern contrast. The engraving depth measurements and the pictures of the engraved surface characteristics were made with a Reichert Research Metallograph MeF No. 300/747.

4.1.4 Results and Discussion

Effect of illumination intensity and exposure time. The equations for the current multiplication upon illumination utilize the induced photovoltage rather than the light intensity. Muller (Ref. 25) indicates the relationship between photovoltage and light intensity in a graphical manner.

Rather than attempt a detailed analysis based on physical principles, an empirical relationship between the engraving depth, x, illumination intensity, I, and engraving time, t, of the following form was assumed.

$$x = kt^{n} \ln I/I_{o}$$

where k, n, and I_o are parameters determined from measurements. The effects of light intensity and engraving time for the 0.5 to 1.5 Ω-cm are indicated in Figs. 5 and 6. The effect of time at 1 light intensity is also indicated for the 190 to 225 Ω-cm material in Fig. 6, and engraving depth versus percent transmittance in Fig. 7 (see Fig. 11). The data presented in these figures indicates that the depth of the engraving on the low-resistivity sample can be represented empirically by the equation

$$x = 0.0625\, t^{1.18} \ln I/1.6$$

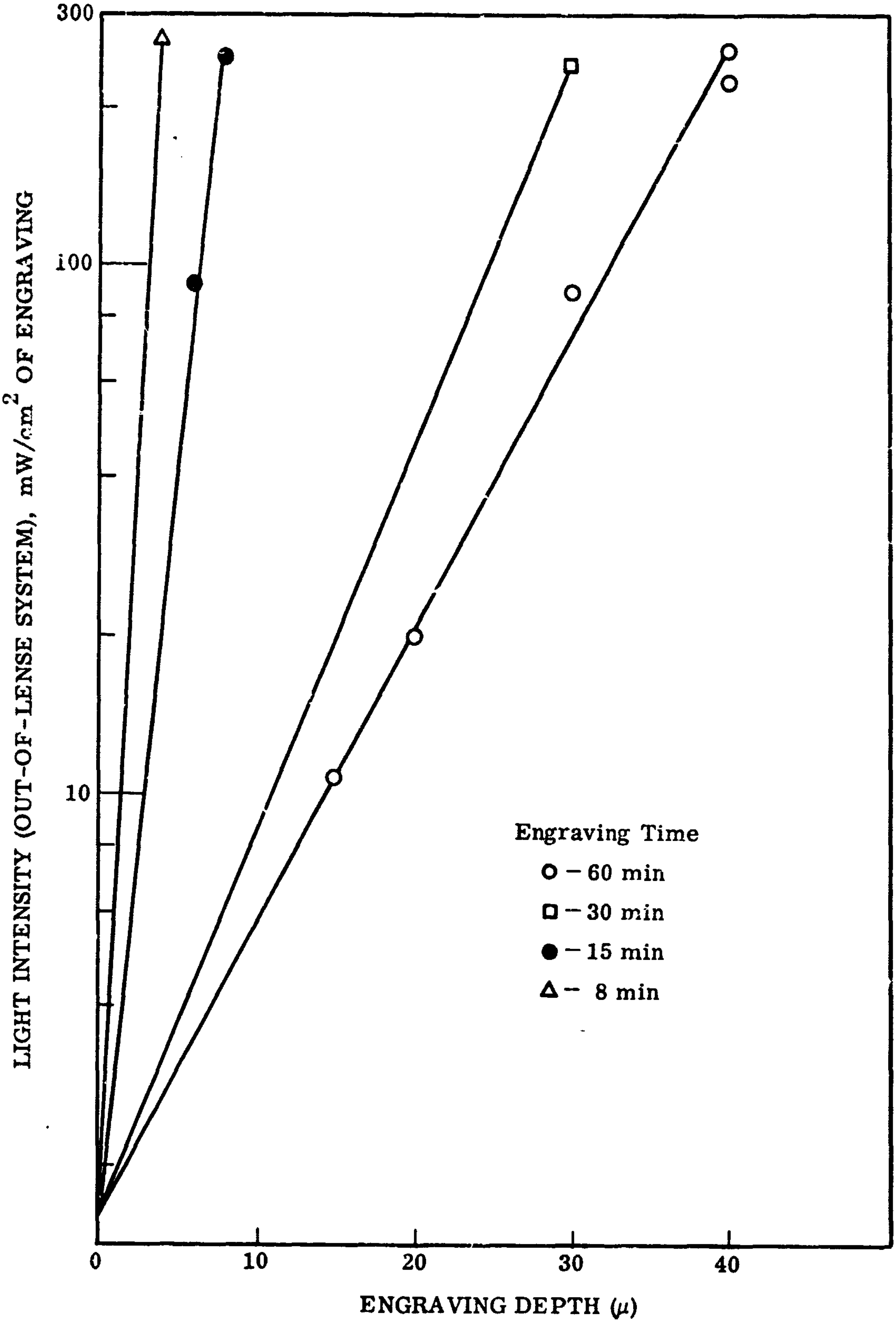

Fig. 5 Effect of Light Intensity Upon the Engraving Depth in 0.5 to 1.5 Ω-cm, n-Type Silicon Oriented in the 1-1-1 Plane

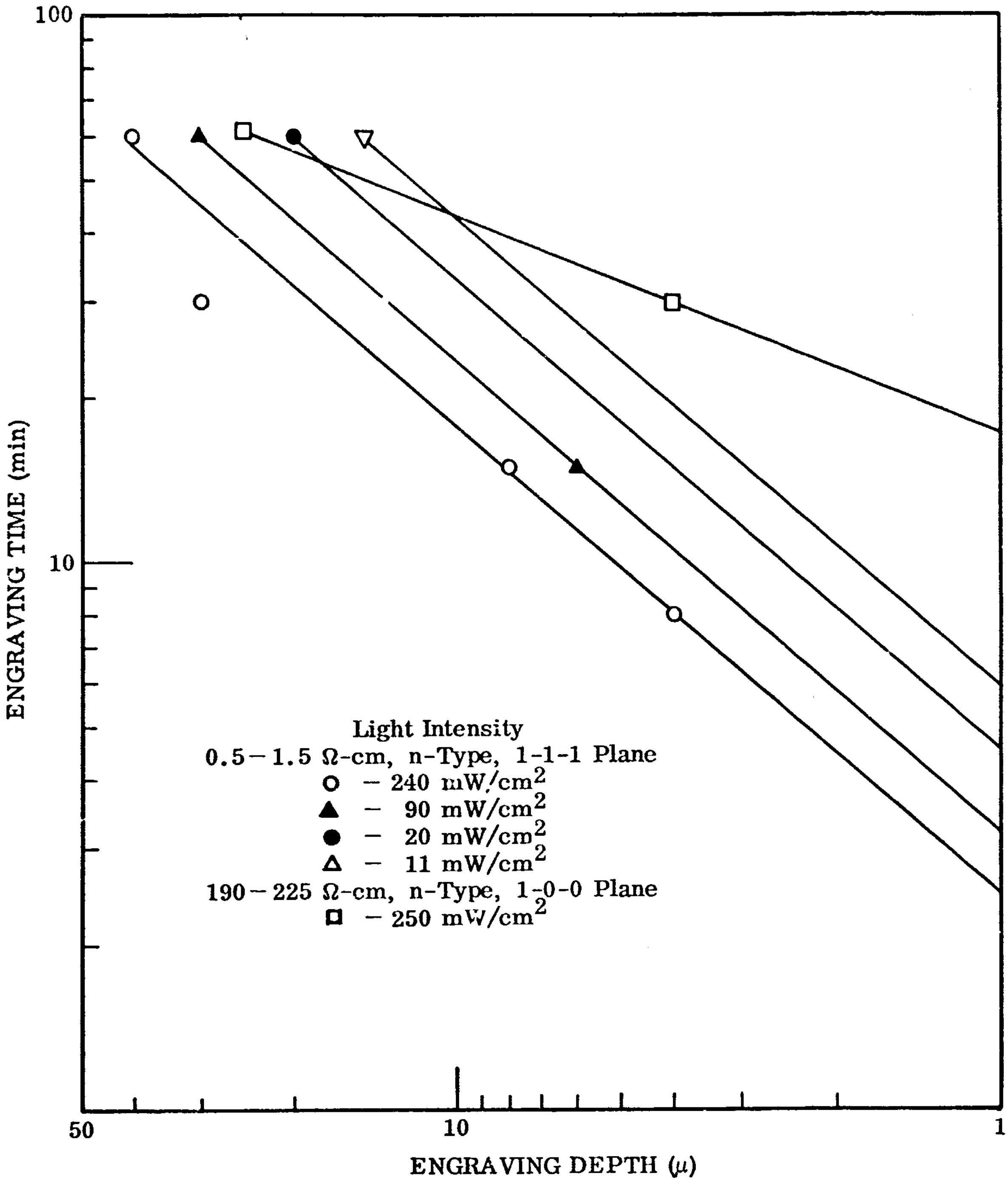

Fig. 6 Effect of Engraving Time Upon the Engraving Depth in n-Type Silicon

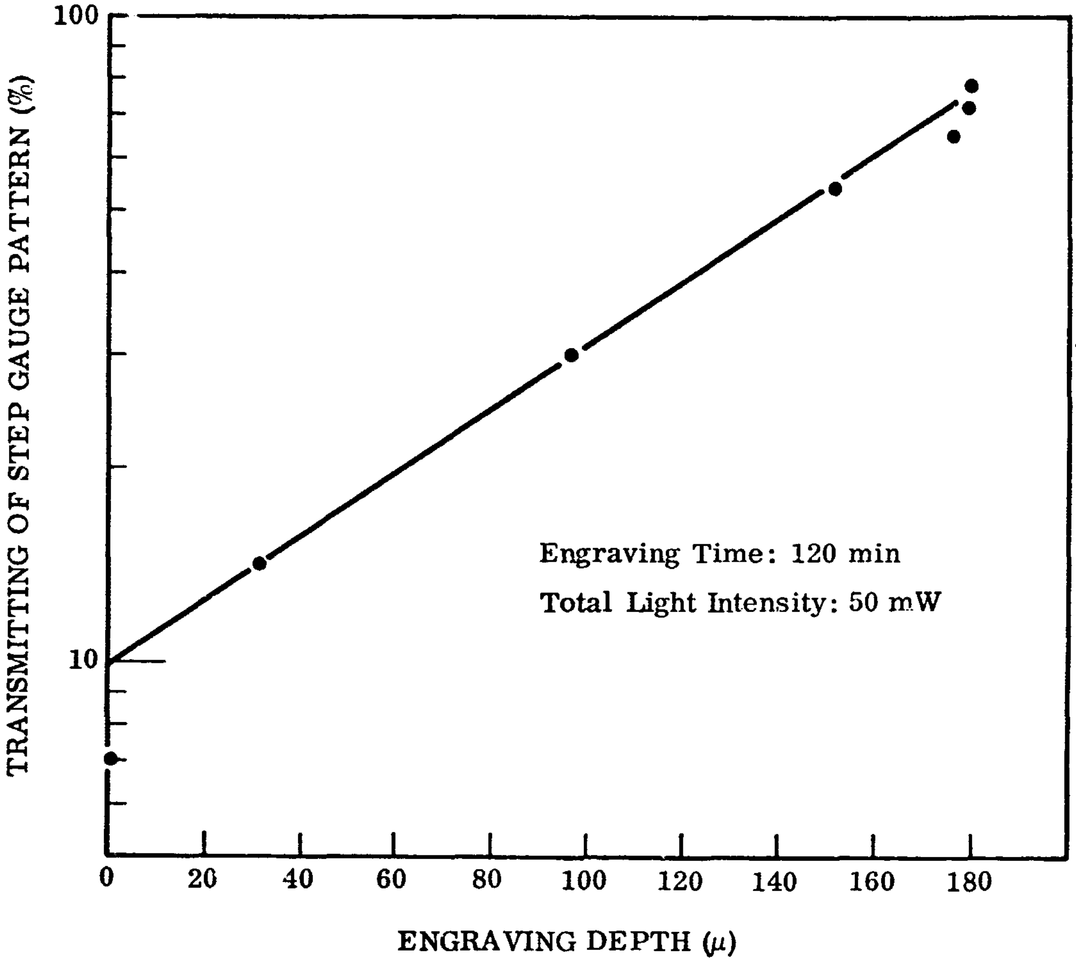

Fig. 7 Effect of Light Intensity Upon the Engraving Depth in 190 to 225 Ω-cm, n-Type Silicon Oriented in the 1-0-0 Plane

The depth of the engraving on the high resistivity material can be represented by the equation

$$x = 4.91 \times 10^{-4} t^{2.53} \ln I/54.5$$

The etch structure obtained on the low-resistivity material and the high-resistivity material is pictured in Figs. 8 and 9, respectively. The surface of the low-resistivity material is quite similar to that obtained by Braun (Ref. 27) and may be due to the effect of orientation although Braun does not indicate the orientation of his material. The surface has the characteristic appearance of terraces developed because of different etch rates of the crystal planes (Ref. 3). However, similar results have been obtained when dislocations are present (Ref. 2). Thus, the specific cause of the terraces is in doubt although the large amount of material removed during the chemical polishing tends to favor the orientation explanation. These terraces result in a nonuniformity of depth amounting to at least 10 μ.

The etch structure obtained on the high-resistivity material resembles very closely (initially) the pits produced by dislocations. However, these pits, with continued engraving, become very concentrated as indicated in Fig. 9. Whether this is due to dislocations or to orientation is not known. However, the results, in terms of the application, are good. The nonuniformity of the surface is microns or less and quite promising as a suitable substrate.

<u>Effect of the optical system on the resolution of the engraving.</u> The 190 to 225 Ω-cm material was used. Engraving was performed with the f4.5 lens and the f1.9 lens. The focusing technique was poor so that a good focus of the pattern on the substrate was difficult if not impossible to obtain. The sample substrate was suspended in Dash etch in a 2-in. polystyrene box at a distance of about 4 mm from the side of the box facing the illumination.

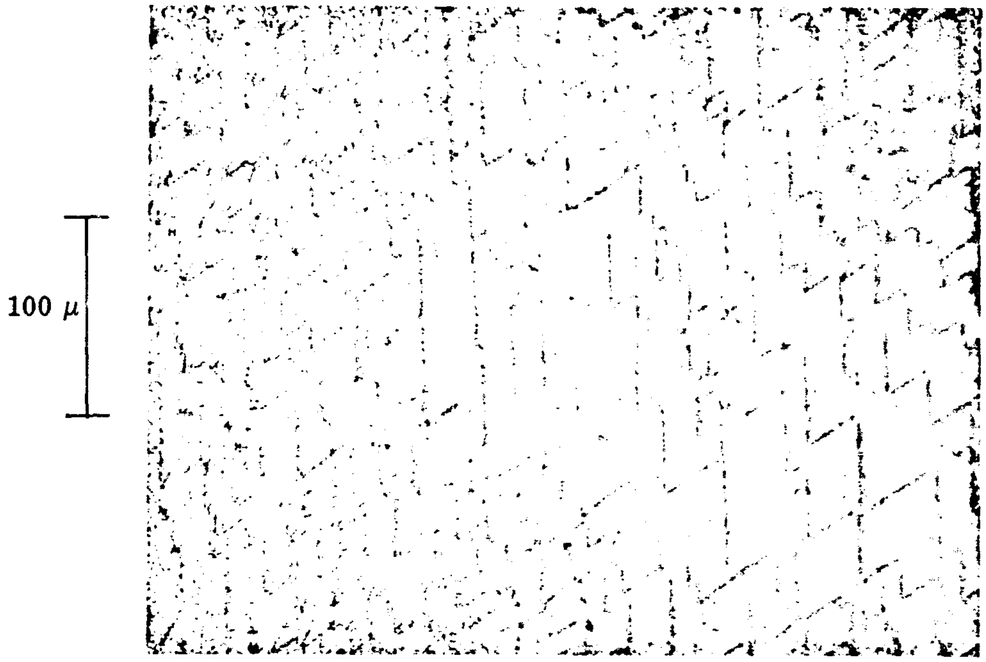

Fig. 8 Terraces Developed on 0.5 to 1.5 Ω-cm n-Type Silicon Oriented in the 1-1-1 Plane. Engraved 1 hr in Dash etch with 240 mW/cm^2 illumination

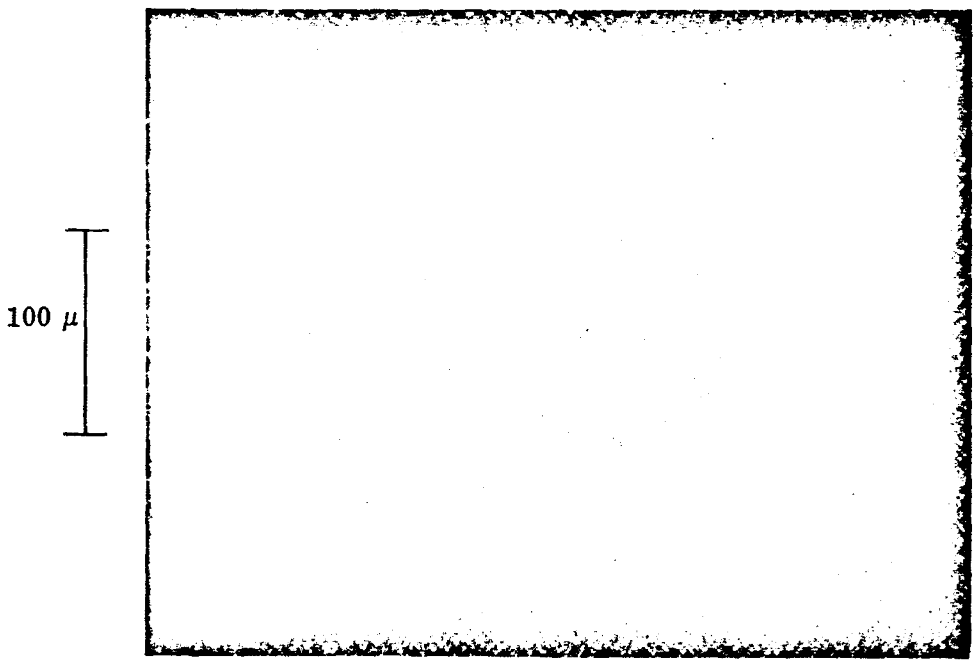

Fig. 9 Pits Developed on 190 to 225 Ω-cm n-Type Silicon Oriented in the 1-0-0 Plane. Engraved 1 hr in Dash etch with 250 mW/cm^2 illumination

The kind of result obtained with the focusing chart and the f4.5 lens is indicated in Fig. 10. The reduction to the sample was 6.43, the total light intensity was 29 mW, and the engraving time was 1 hr. Slightly more than one half of the chart is on the sample. A fringe effect on resolution of about 12 μ is indicated. The only portions of the chart which cannot be resolved are those portions consisting of 5-mil dots spaced 5 mils apart (black dots on clear area). However, there is a "cross" effect in these areas which is not present in the other areas and which can be said to be indicative of the dots. The 5-mil alternating black and clear lines can be resolved. There is an overall etch, but the depth of etch under the center of the black lines is about 4 μ compared to about 30 μ under the clear lines. On the sample these lines are each about 19 to 20 μ in width. The total depth of the engraving was about 30 μ with a horizontal resolution of better than 12 μ.

The results obtained with the photographic step gauge are indicated in Fig. 11. The reduction of the image was 6.6, the total light intensity was 50 mW, and the engraving time was 2 hr. The first step – black – was not visible, while the second step was slightly visible due to a few et[illegible], but with no overall change in the surface. The third step was about 2 μ lower than the second step, the fourth step about 30 μ lower than the third step, the fifth about 65 μ, the sixth about 55 μ, the seventh 25 μ, and no change of depth (by step) was apparent for the eighth and ninth steps although there did appear to be a slight continuous variation. In the areas of strong light, after about the sixth step, etching was apparent on the back of the sample, which was about 1-mm thick. The apparent fault down the center of the sample is due to light reflected from a misplaced auxiliary part. The percent transmittance of the step gauge was determined by densitometer to be 0, 0.7, 6, 14, 30, 54, 65, 72, 78.

The results obtained with the f1.9 lens and the focusing chart and a reduced chart (5.29 reduction) are indicated in Figs. 12 and 13. The total reduction was 45 using the reduced chart (Fig. 12) and the reduction using the focusing chart was 8.2 (Fig. 13). The poor resolution of this lens is apparent, both from the broad halo around the engraved area, and from the complete loss of the fine lines in the focusing

⊢⊣ 1000 μ

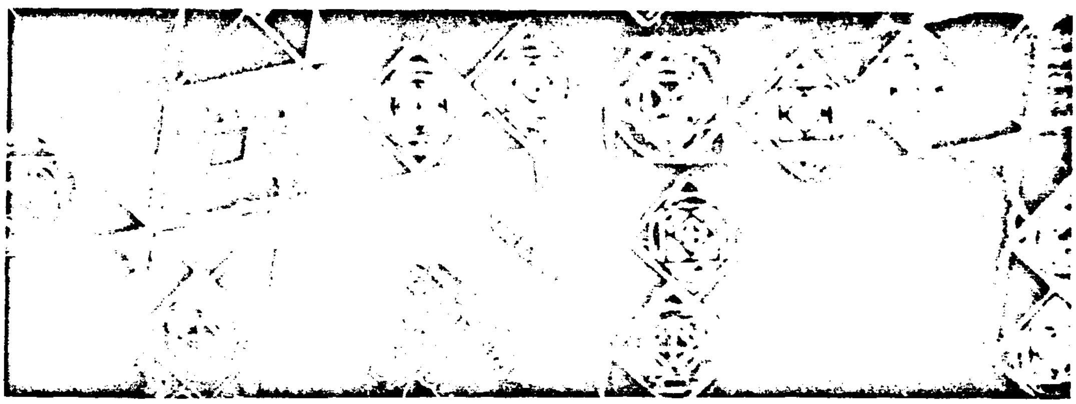

Fig. 10 Pattern Engraved on 190 to 225 Ω-cm n-Type Silicon (1-0-0 Orientation) in Dash Etch for 1 hr With a Total Light Intensity of 29 mW. Slightly more than one-half the pattern is on the silicon

⊢⊣ 10 mm

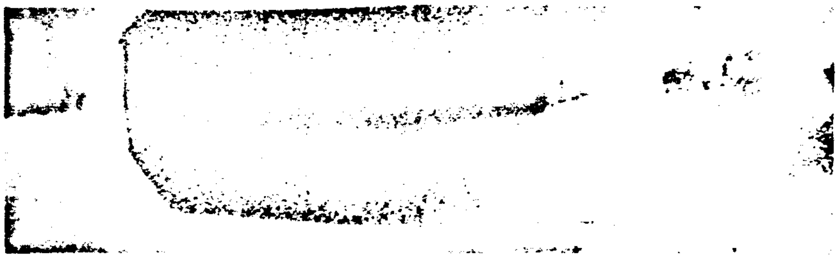

Fig. 11 Photographic Step Gauge Engraved on 190 to 225 Ω-cm n-Type Silicon (1-0-0 Orientation) in Dash Etch for 1 hr With a Total Light Intensity of 50 mW

Fig. 12 Reduced Pattern Engraved on 190 to 225 Ω-cm n-Type Silicon (1-0-0 Orientation) in Dash Etch for 50 min at a Total Light Intensity of 6.4 mW. A low quality f1.9 lens was used

Fig. 13 Pattern Engraved on 190 to 225 Ω-cm n-Type Silicon (1-0-0 Orientation) in Dash Etch for 2 hr at a Total Light Intensity of 2.3 mW. A low quality f1.9 lens was used. (For comparison see, Fig. 10)

chart (Fig. 13). The total light intensity for the reduced chart (Fig. 12) was 6.4 mW and the engraving time was 50 min. The negative was not black and clear, but had a density, in the dark areas, comparing to the fourth or fifth step on the step gauge. The results for the step gauge indicate that the dark areas should be etched to about one-third to one-half the depth of the clear areas. The actual depths were about 26 μ and about 16 μ.

4.1.5 Summary

The depth of an engraving (or etch) using the photoengraving technique can be represented by the equation

$$x = 0.0625\, t^{1.18} \ln I/1.6$$

for the low-resistivity material, and by the equation

$$x = 4.91 \times 10^{-4}\, t^{2.53} \ln I/54.5$$

for the high-resistivity material.

The high-resistivity material gives an etched surface which is much more uniform and more applicable to photoengraving with high resolution.

The lens system must be good in order to obtain good resolution.

The application under consideration is the engraving of an image at a scale of 1 in. equal to 1 mile with a resolution of about 1 ft or 5 μ on the engraving. The present system gives a resolution of a little better than 12 μ or 2.5 ft. Better resolution can probably be obtained. However, provided there are no sharp or deep precipices in the original, the present system can probably be used to obtain an engraving which has an effective resolution approaching that desired with proper corrections incorporated in the pattern.

The results obtained indicate several factors which probably affect the resolution of the engraving and the degree to which it reproduces the original. Some of these factors are:

- The pattern: the engraving can, of course, be no better than the pattern.
- The lens system: good lenses must be used to obtain sharp images with good resolution. The depth of field (or focus) of the lenses should be compatible with the depth of the engraving.
- The light and type of light: the use of monochromatic light of a particular wavelength should greatly decrease the possibility of scatter and diffraction through the pattern and lens system, and through the cell wall and engraving solution.
- The cell window: the window material must not only be inert toward the engraving solution, but must also have good optical properties.
- The diffusion length and other properties of the injected electron-hole (pairs) and/or the resistivity of the material: this study indicates that high-resistivity 1-0-0 oriented material is desirable. However, highly doped high-resistivity material, low-resistivity 1-0-0 oriented material, or high-resistivity 1-1-1 oriented material may give similar results – and it may be possible to approach the engraving rates of the low-resistivity material.
- Material crystal form: polycrystalline or monocrystalline material, and the crystal orientation, may affect the engraving rate and the type of surface obtained.
- Technique: the manipulative technique becomes quite critical in obtaining the degree of resolution desired. A very stable system and critical means of focus and alignment is a necessity.

4.1.6 Future Work

The feasibility and applicability of this technique has been adequately demonstrated. The resolution now obtained can be incorporated in the design of a pattern if sharp height changes are not required.

Future work should include general improvement of the lens and window system, and sample, pattern, and lens alignment and/or orientation. Tests should include the study of the effects of the type of light, the depth of the sample in the engraving solution, the effect of highly doped, high-resistivity material, the effects of crystal orientation, the effects of polycrystalline versus monocrystalline material, and the effects of the material (i.e., silicon, germanium, and other photosensitive materials).

4.2 PHOTO SUBLIMATION

Photographs of part of the apparatus used in these experiments and a typical result are shown in Fig. 14. In these experiments a number of materials were selected for their property of subliming at moderate temperature and for their absorption of visible light. The materials used were iodine, phthalocyanine, and copper phthalocyanine; the latter two being organic compounds.

The material was compressed in a laboratory pellet press to produce a smooth-surfaced pellet and the pellet placed in an evacuated chamber on a platform through which liquid nitrogen could be circulated for cooling. As Fig. 14a and 14b show, light from an intense light source was collected by a condensing lens system and passed through a cross-hair aperture before being focused by an objective lens onto the surface of the pellet. Figure 14c shows the cross-hair image on a pellet through the flat distortion-free glass top of the vacuum system. In operation the vacuum system could be covered so that only light from the focused image would fall on the pellet.

Experiments were performed with a continuous light source (a spotlight), a flash lamp, and a Q-switched laser light source. The best results were achieved with the flash lamp, whereas no results at all were obtained with the pulsed laser and only rudimentary results with the spotlight. None of the results achieved were competitive with the photochemical method in respect to resolution and ease of handling so that the experiments were stopped before many aspects were investigated and before results were achieved which merited quantitative work.

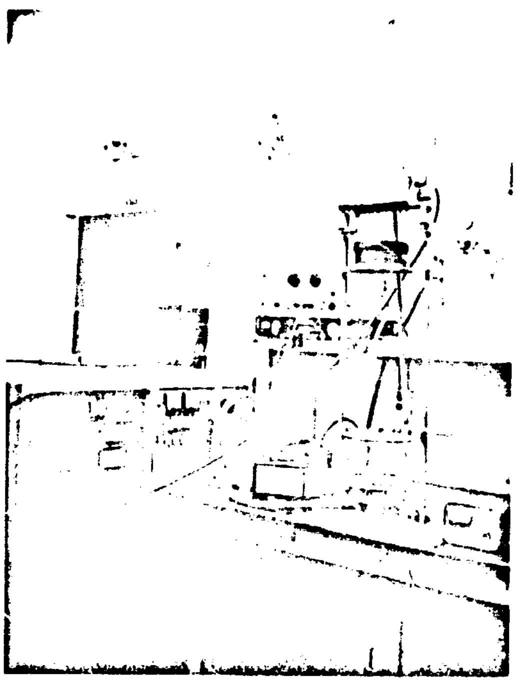

a.

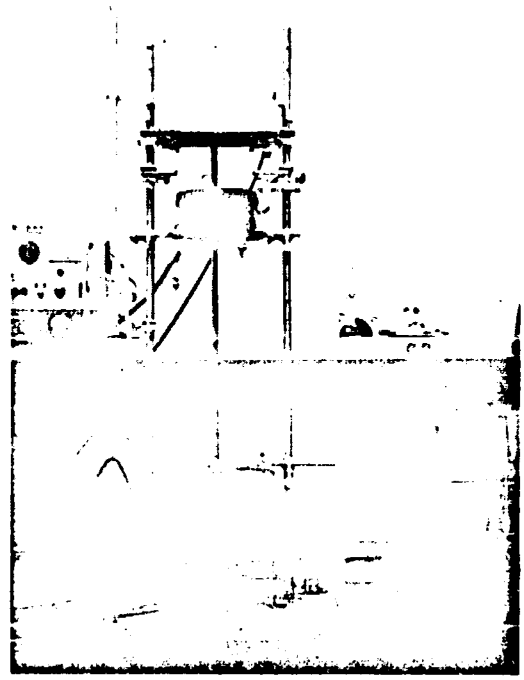

b.

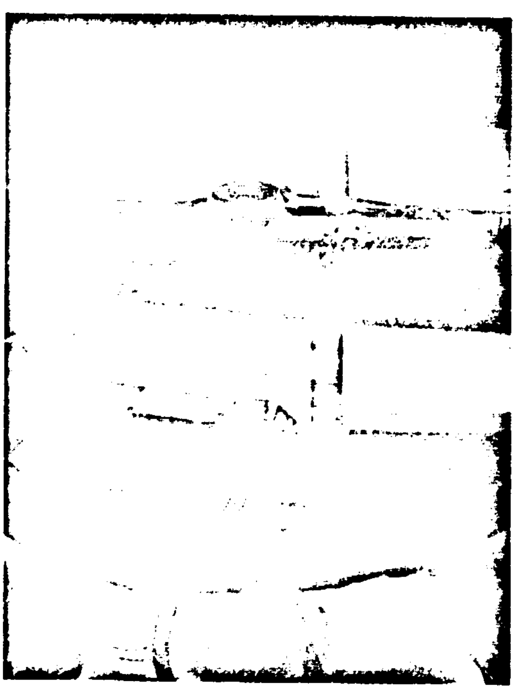

c.

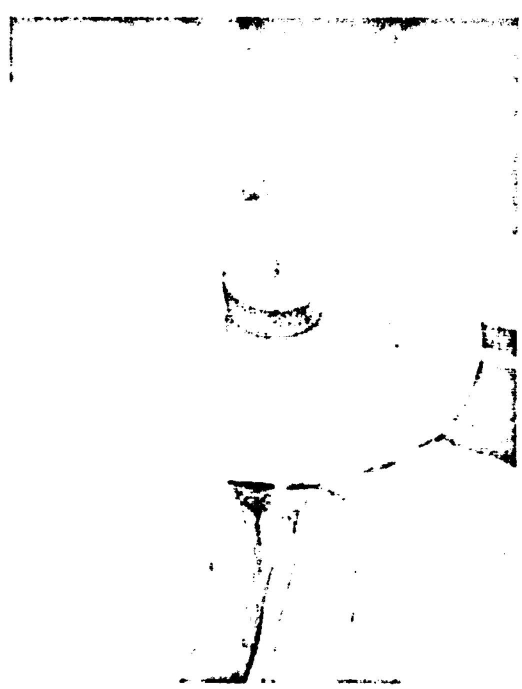

d.

Fig. 14 Experiments in Photo Sublimation

Figure 14d shows the result of pulsed light on an uncooled iodine pellet. The lines are about a millimeter wide. The light source was a xenon flash lamp which was excited with a 10, 000-J pulse of about 1.5 msec duration once a minute for a total of 20 flashes. Notice that the surface of the pellet is no longer smooth even in areas where light was not present. This was probably mostly due to the fact that the iodine pellet was pressed from a coarsely ground rather than a fine-grain powder. Ideally, the particle size should be much less than the desired 1-μ depth resolution as the sublimation from the surface would tend to follow particle boundaries.

Resolution in Fig. 14d also appears to be rather poor. The edges are rounded off. This is a similar effect to the softening of the corners of a cube of butter fresh from the refrigerator.

Both the coarse texture and the loss of resolution were greatly improved by an experiment with iodine in which the pellet was replaced by a glass slide. The base was cooled, and at the same time a small amount of iodine elsewhere in the vacuum jar was warmed to create an iodine vapor which then began to deposit on the cold glass slide. As the deposit built up, the flash lamp was operated to image the Burke and James focusing chart (Fig. 10) on the deposit surface. A much finer texture was realized and the resolution was very much improved.

The iodine experiments always suffered from the fact that any image produced lost resolution with time due to continued sublimation. It is possible that techniques could be developedfor quickly replicating an iodine surface. However, the tests using the phthalocyanines were an attempt to duplicate the process in a more stable material. Using the 10, 000-J flashlamp, images were formed on the surface of the phthalocyanine pellets but the surfaces were not really contoured. Microscopic examination showed that where the surface was struck by light it was crazed with many tiny cracks, much as is the mud bottom of a dry lake. This may have indicated the vaporization of included water.

To summarize, the sublimation experiments were only successful with iodine and showed the best resolution when the image was formed in a fine-grained deposit forming from the vapor. The flashlamp imaging was most successful because a large amount of energy was delivered to the surface in a time which was short compared to the time required for heat to diffuse throughout the material. Consequently, the local temperature rise followed the light pattern and vaporization took place primarily where the light was present.

Section 5
SURFACE CONTOUR MEASUREMENT

A surface measurement method is needed whether the surface is formed by deterministic or random means. In either case, it will be necessary to find out what has been achieved by the surface-forming process.

5.1 PROFILING

There are available a few very precise surface-profiling instruments. These draw a finely tipped diamond stylus across a surface in a straight line and measure the vertical displacement of the stylus as this is done. Figure 15 is an example of a section of recording made by the Clevite-Brush Surfanalyzer 150 of a piece of textured glass later used in initial scattering measurements. Figure 16 shows a cross section of the probe tip. The radius of 2.5 μ allows the probe to follow closely spaced surface irregularities. The 90-deg shank angle limits surface slopes to 100% but since the ocean surface replica will have a maximum of 20%, this is satisfactory. The sensitivity of measurement is to 1 μ-in., well beyond the 1 μ (40 μ-in.) required. Such sensitivity requires good vibration isolation.

When a three-dimensional surface is measured using profiling, a number of profiles are taken at different locations and at different angles and the results averaged to find the spectrum of the surface. The directional spectrum can be obtained by profile measurements in different directions.

5.2 PHOTOGRAPHING INTERFERENCE MICROSCOPE

In this method, monochromatic light produces alternate light and dark bands (fringes) in a microphotograph of the surface. Figure 17 is an example. Each successive band

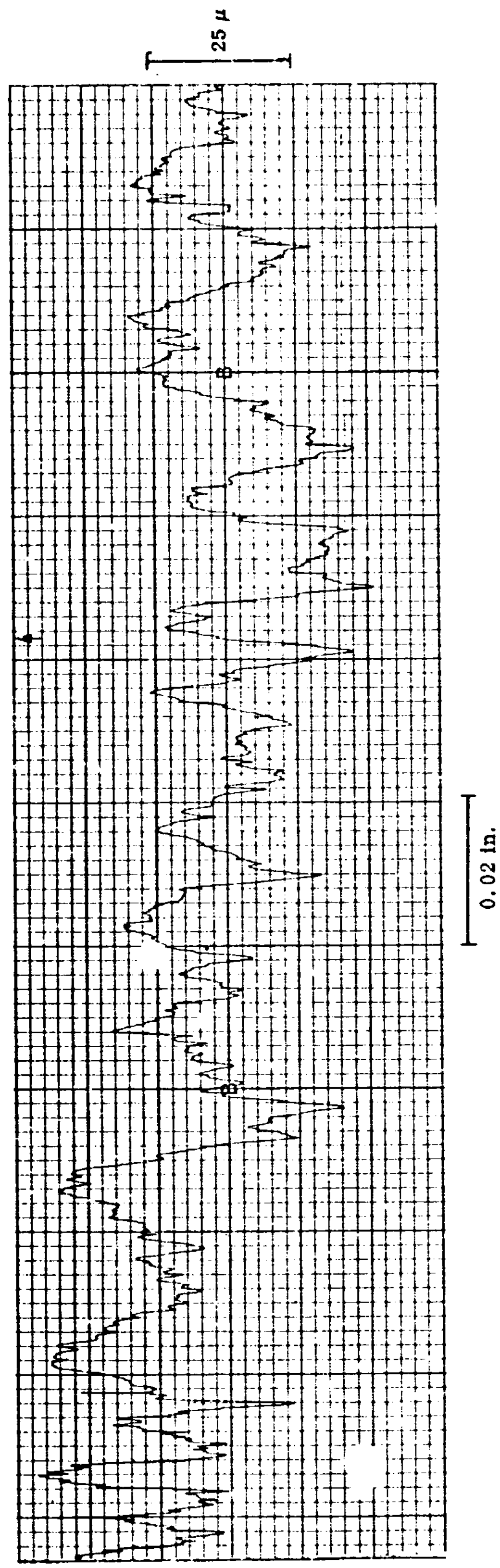

Fig. 15 Profile of Roughened Glass

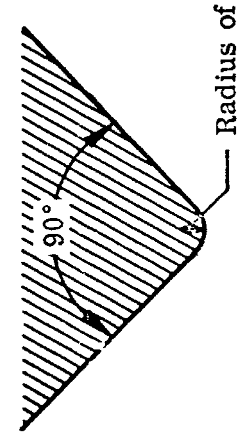

Fig. 16 Profiler Tip

Fig. 17 Interference Photomicrograph of a Silicon Epitaxial Film Having a Lapped Depression

represents a change in surface height equal to the wavelength of light being used. Therefore, the vertical resolution is about 0.5 μ. A photo is profiled either by hand or by machine. Often the surface must be stained in order to obtain satisfactory photographs. Also,some human interpretation is needed when the surface goes through maxima and minima.

5.3 OTHER METHODS

Two other methods were considered during the study. In one, an acoustic planewave incident on the surface to be measured would produce diffraction patterns on reflection. These would be measured by an acoustic detector. An analysis showed that this method was not able to cover the range of spatial frequencies of interest.

In another method studied, a film plate is placed in contact with the back surface of the target and irradiated by x-rays passing through the target. This would give an exposure on the film inversely proportional to the exponential of the target thickness. Scanning the film with a microdensitometer and applying the appropriate correction factors would then give the target height function. One test of this method was made with negative results.

Section 6
SIMULATION EXPERIMENT

Figure 18 shows the experimental setup for scattering experiments in its initial form. In Fig. 18a, the target appears as a 1-in.-square white object at the far end of the H-beam bench. It is mounted on a turntable which produces motor driven or manual rotation and/or translation. Potentiometers attached to the turntable provide voltages which show target angle or translation.

In Fig. 18b may be seen the 10.6-μ laser, the beam chopper, the detector, detector amplifiers, and recorder. The laser beam diameter is 2 mm with a beam divergence of two milliradians as it emerges from the laser. The toothed chopper wheel produces a square-wave modulation of the transmitted beam at about 1200 Hz and by means of a small light and photocell produces a synchronous reference voltage for the detector amplifier. The detector is on the left in Fig. 18b, mounted on an adjustable stand. It has an adjustable aperture which is set so that the detector field of view includes only slightly more than the target. In this way, secondary scattering of laser energy first scattered from the target does not enter the detector.

The detector itself is a gold-doped germanium semiconductor operated at liquid nitrogen temperature. Gold-doped germanium is not the optimum detector for this wavelength and later measurements are planned with a copper-doped germanium detector. The detector output consists of (a) a dc component due to the temperature of the target and its surroundings, (b) an ac component at 1200 Hz which is the scattered 10.6-μ laser signal, and (c) noise components due to thermal noise of the detector resistance and the quantum nature of the background noise.

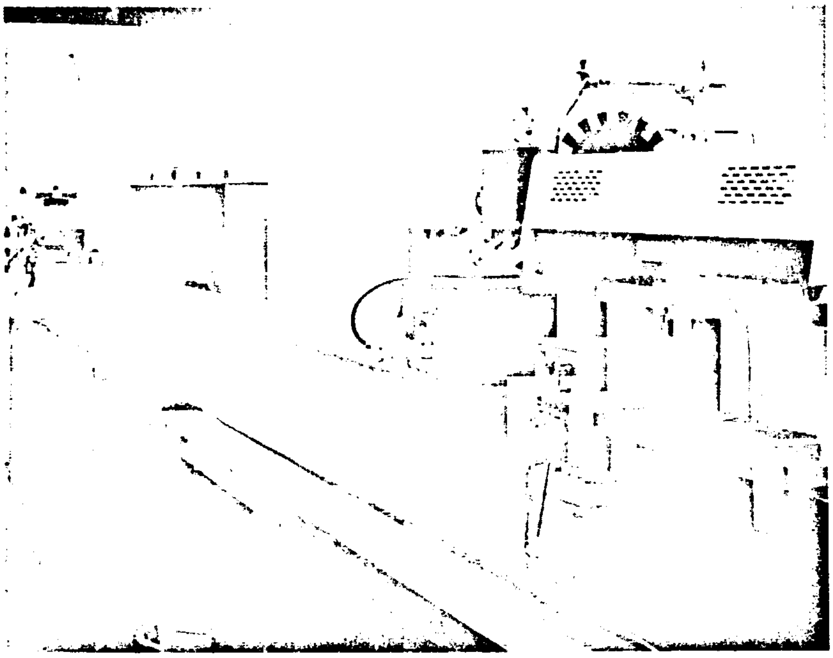

a. Target Turntable at Far End of the Bench

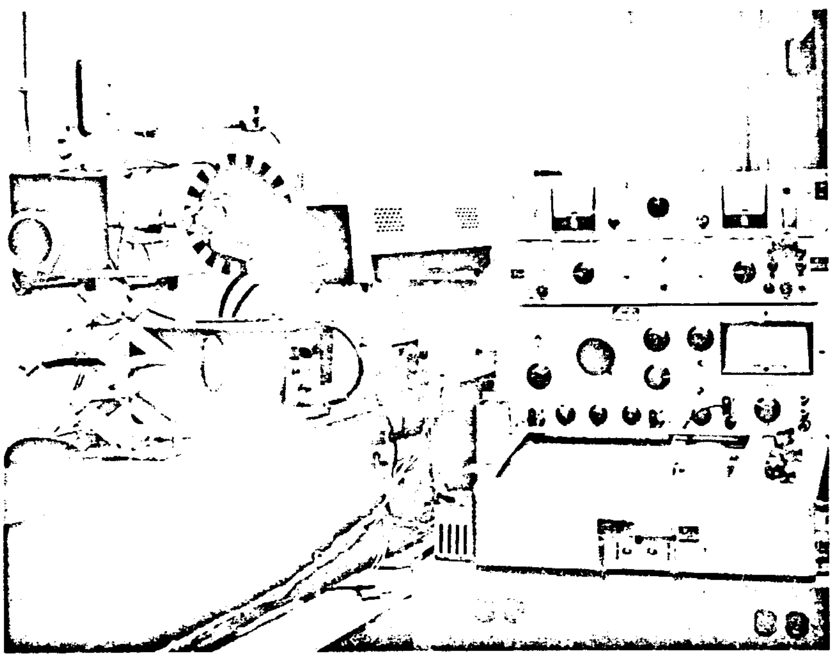

b. Laser, Chopper, Detector, Detector Amplifiers, and Recorders

Fig. 18 Scattering Simulation Equipment

Because the desired target-scattered portion of the detector output is small compared to the noise output, the detector output is delivered to a Lock-In Amplifier. Here the signal is amplified and then synchronously demodulated using the 1200-Hz reference voltage. The synchronous demodulator output is passed through a low-pass filter having a response time as long as 10 sec. It is then plotted as the ordinate on an X-Y plotter where the abscissa is the target turntable angle or position. Figure 19 is an example of a scattering curve as a function of incidence angle. The target is the aluminized glass whose profile is shown in Fig. 15. This is a rather rough surface as indicated by the width of the scattering curve. In the figure, the two upper curves are reruns of the same condition except that the laser power output was repeaked after the first run. The lower curve is a retrace of the turntable between runs with laser power off. It therefore indicates the amount of noise in the detector system. The data runs could not be expected to repeat within that amount of noise. This indicates a need for improved detector signal-to-noise ratio which should be achieved when the copper-doped germanium detector is used.

The raw data of Fig. 19 can be averaged for the two runs and the two directions of incidence angle to produce the scattering curve shown in Fig. 20. Here the scattered signal is plotted in dB relative to the normal incidence signal. Evidently satisfactory data can be obtained in this manner even with the present experimental equipment for a considerable range of targets. The target which provided these data is one of the roughest targets one would expect to use in the experiments and therefore scatters the energy more widely than most targets.

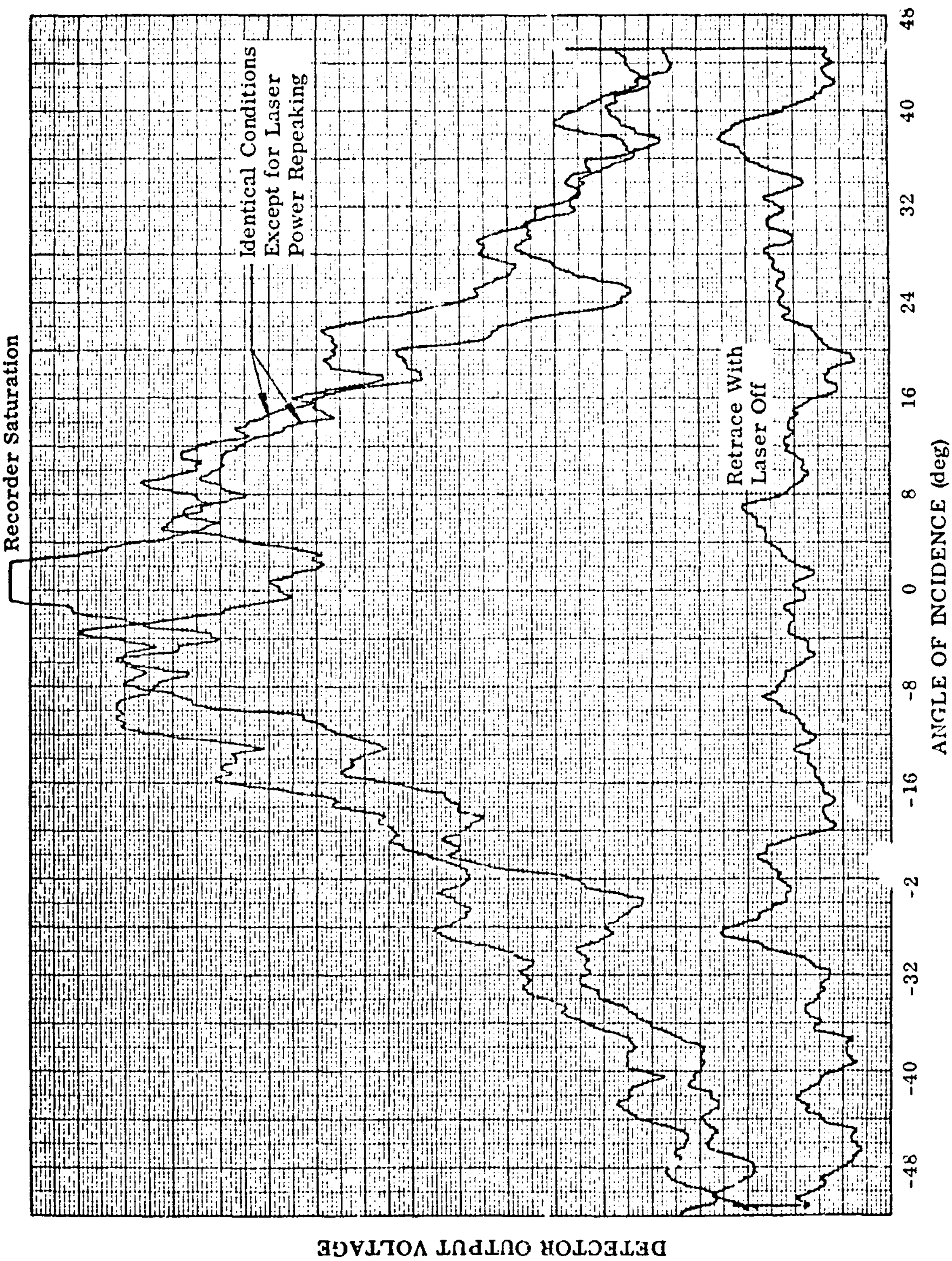

Fig. 19 Raw Scattering Data From Aluminized Rough Glass

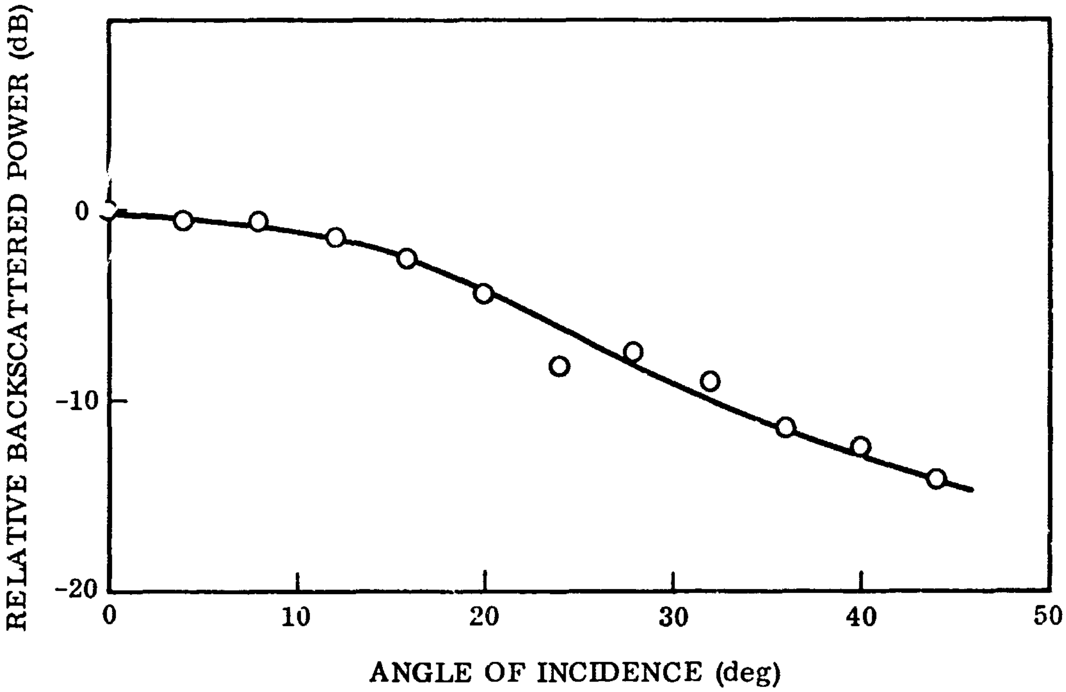

Fig. 20 Backscattering Function for an Aluminized Glass Random Target

Section 7
CONCLUSION

This report has examined the principal factors which determine the feasibility of laboratory simulation of satellite-borne microwave sea-surface scattering by means of wavelength and target dimensional scaling. The most promising approach is the use of 10.6-μ laser radiation to simulate low microwave frequencies.

Experiments in target fabrication techniques have indicated that light-activated chemical etching of silicon can produce sufficient surface detail and extent to represent a square mile of ocean surface when the frequency being simulated is 500 MHz.

A laboratory simulation facility has been established which consists of a 10.6-μ CO_2 laser, a cryogenic detection system, a target positioning turntable, and recording devices. Initial scattering measurements have been made from random surfaces to prove out the equipment.

Section 8
REFERENCES

1. P. Beckman and A. Spizzichino, The Scattering of Electromagnetic Waves From Rough Surfaces, New York, Macmillan, 1963
2. J. D. de Lorenzo and E. S. Cassedy, "A Study of the Mechanism of Sea Surface Scattering," IEEE Trans. on Antennas and Propagation, Vol. A-8-14, Sep 1966, pp. 611–620
3. A. K. Fung and R. K. Moore, "The Correlation Function in Kirchoff's Method of Solution of Scattering of Waves from Statistically Rough Surfaces," J. Geophys. Res., Vol. 71, Jun 1966, pp. 5181–5190
4. R. B. Ward, Some Considerations in the Design of a Satellite Radar-Altimeter/ Sea-Surface-Sensing Device, L-86-67-3, Lockheed Missiles & Space Co., Palo Alto, Calif., Jul 1967
5. J. R. Huynen, Radar Backscatter from Distributed Targets with Emphasis on Polarization Dependence, L-86-67-2, Lockheed Missiles & Space Co., Palo Alto, Calif., May 1967
6. W. Marks, Application of Airborne Radar Backscattering to Measurement of Sea State, Oceanics, Inc. Report 0I-64-17, Apr 1964
7. F. H. Maltz, The Statistics of Microwave Scattering from the Ocean, L-86-67-1, Lockheed Missiles & Space Co., Palo Alto, Calif., May 1967
8. A. N. Fried, "Radar Reflection Characteristics of Terrain and Water Surfaces – An Annotated Bibliography," LMSC Literature Search LS 67-32, Dec 1967
9. W. Boles, A. K. Fung, and R. K. Moore, "Bistatic Measurements of Acoustic Waves Scattered from a Statistically Rough Known Surface at 1 MHz," URSI 1966 Fall Meeting, Stanford, Calif.

10. H. V. Hance and W. R. Ramsay, Status Report and Program Plan – Simulation of Radar Signal Scattering from Terrain (Secret), LMSC-B038099, Lockheed Missiles & Space Co., Palo Alto, Calif., 17 Jul 1967

11. W. L. Floyd and T. J. Lund, "Scatterometer Program," Supplement to IEEE Trans. on Aerospace and Electronic Systems, Vol. AES-2, No. 6, Nov 1966, pp. 323–328

12. Techniques of Microphotography, Kodak Bulletin No. P-52, Eastman Kodak Co., Rochester, N. Y.

13. "A Guide to Total Surface Measurement and the American Standard ASA B46.1-1962 Surface Texture," Brush Instruments Division, Clevite Corp., El Monte, Calif.

14. Ford Park, "Nontraditional Machining," International Science and Technology, Nov 1963, pp. 22–35

15. H. F. Brandli et al., "Microdrilling Ruby Watch Jewels," Laser Focus, May 1967, pp. 26–32

16. C. M. Adams and G. M. Hardway, "Fundamentals of Laser Beam Machining and Drilling," Trans. IEEE-IGA, Mar–Apr 1965, pp. 90–96

17. Gerhard Rauscher, "UBL 5001, A Versatile Micromachining Laser," Siemens Review, Nov 1967, pp. 432–435

18. R. F. Bunshah, "High Power Electron Beams," International Science and Technology, Apr 1962, pp. 30–38

19. W. E. Glenn, "Thermoplastic Recording, A Progress Report," Journal SMPTE, Aug 1965, pp. 663–665

20. J. H. Altman, "Pure Relief Images on Type 649-F Plates," Applied Optics, Oct 1966, pp. 1689–1690

21. W. H. Brattain and C. G. B. Garrett, Bell System Tech. J., Vol. 34, 1955, A129

22. H. C. Gatos, The Surface Chemistry of Metals and Semiconductors, John Wiley and Sons, Inc., New York, 1959, pp. 218 – 222, 390 – 395

23. Holmes, The Electrochemisty of Semiconductors, Academic Press, New York, 1962, pp. 97 – 99, 175, 181, 299, 302, 311, 316, 326 – 327

24. D. R. Turner, J. Electrochem. Soc., Vol. 107, No. 10, 1960, pp. 810 – 816

25. G. R. Booker and Stickler, J. Electrochem. Soc., Vol. 109, No. 12, 1962, pp. 1167 – 1171

26. R. S. Muller, Ibid, pp. 1195 – 1197

27. J. H. Braun, J. Electrochem. Soc., Vol. 108, No. 6, 1961, pp. 588 – 589

28. D. D. Evers (to Philco), U.S. Patent 2, 767, 137, 16 Oct 1956

29. F. J. Biondi, Transistor Technology, Vol. III, D. Van Norstrand Co., Inc., Princeton, 1958, p. 134

30. W. C. Dash, J. Appl. Phys., Vol. 27, 1956, p. 1193